CMLS, Cell. Mol. Life Sci. 59 (2002) 882–893
1420-682X/02/050882-12 $ 1.50 + 0.20/0

CMLS Cellular and Molecular Life Sciences

Research Article

Chronic gestational exposure to ethanol impairs insulin-stimulated survival and mitochondrial function in cerebellar neurons

S. M. de la Monte* and J. R. Wands

Departments of Medicine and Pathology, Pierre Galletti Research Building, Rhode Island Hospital, 55 Claverick Street, Room 419, Providence, Rhode Island 02903 (USA), Fax: + 401 444 2939, e-mail: delamonte@hotmail.com

Received 21 January 2002; received after revision 28 February 2002; accepted 25 March 2002

Abstract. Chronic gestational exposure to ethanol has profound adverse effects on brain development. In this regard, studies using in vitro models of ethanol exposure demonstrated impaired insulin signaling mechanisms associated with increased apoptosis and reduced mitochondrial function in neuronal cells. To determine the relevance of these findings to fetal alcohol syndrome, we examined mechanisms of insulin-stimulated neuronal survival and mitochondrial function using a rat model of chronic gestational exposure to ethanol. In ethanol-exposed pups, the cerebellar hemispheres were hypoplastic and exhibited increased apoptosis. Isolated cerebellar neurons were cultured to selectively evaluate insulin responsiveness. Gestational exposure to ethanol inhibited insulin-stimulated neuronal viability, mitochondrial function, Calcein AM retention (membrane integrity), and GAPDH expression, and increased dihydrorosamine fluorescence (oxidative stress) and pro-apoptosis gene expression (p53, Fas-receptor, and Fas-ligand). In addition, neuronal cultures generated from ethanol-exposed pups had reduced levels of insulin-stimulated Akt, GSK-3β, and BAD phosphorylation, and increased levels of non-phosphorylated (activated) GSK-3β and BAD protein expression. The aggregate results suggest that insulin-stimulated central nervous system neuronal survival mechanisms are significantly impaired by chronic gestational exposure to ethanol, and that the abnormalities in insulin signaling mechanisms persist in the early postnatal period, which is critical for brain development.

Key words. Fetal alcohol syndrome; fetal ethanol effects; central nervous system; insulin; neuronal apoptosis; mitochondria; signal transduction.

Ethanol exposure during development is teratogenic and one of the leading causes of mental retardation in Europe and North America. Heavy gestational exposure to ethanol can cause fetal alcohol syndrome (FAS), which encompasses a broad array of neurologic and systemic lesions including central nervous system (CNS) malformations such as microcephaly, reduced cerebral white matter volume, ventriculomegaly, cerebellar hypoplasia, and disorders of neuronal migration [1]. Experimental models of FAS have demonstrated that the accompanying CNS abnormalities are due to impaired neuronal viability, growth, synaptogenesis, cell migration, cellular maturation, neurotransmitter function, and intracellular adhesion [2–8]. The overall contribution of ethanol abuse to the incidence of neurodevelopmental defects is probably underestimated, since FAS is poorly recognized. Results from experimental animal models suggest that even moderate levels and durations of ethanol exposure during gestation can be neurotoxic, and substantially reduce CNS neuronal populations [9, 10].

* Corresponding author.

Results of in vivo and in vitro experiments have revealed that ethanol-induced neuronal loss is mediated by apoptosis [2, 7, 11–14] and/or impaired mitochondrial function [11, 12, 15, 16]. Although the mechanisms of neuronal loss and impaired function are not completely understood, findings with in vitro exposure models suggest that these adverse effects of ethanol are mediated in part by inhibition of insulin and insulin-like growth factor-1 (IGF-1) signaling [11, 12, 14, 17, 18]. In the developing CNS, insulin and IGF-1 receptors are abundantly expressed [19–21] and intracellular signals transmitted through these receptors modulate neuronal growth, viability, energy metabolism, and synapse formation [20, 22–24]. Therefore, ethanol inhibition of insulin- and IGF-1-stimulated functions may contribute substantially to the cellular abnormalities that cause neurodevelopmental defects.

The stimulatory effects of insulin and IGF-1 are mediated through complex pathways, beginning with ligand binding and activation of intrinsic receptor tyrosine kinases [25, 26], which phosphorylate specific cytosolic molecules, including two of the major substrates, insulin receptor substrate types 1 (IRS-1) and 2 (IRS2) [27–29]. Tyrosyl phosphorylated IRS (PY-IRS) molecules transmit intracellular signals that mediate growth, metabolic function, and viability by interacting with downstream src-homology 2 (SH2)-containing proteins through specific motifs located in their C-terminal regions [27–29]. For example, the ^{613}YMPM and ^{942}YMKM motifs of IRS-1 bind to the p85 subunit of phosphatidylinositol-3 kinase (PI3 kinase) [30, 31], which inhibits apoptosis by activating Akt/protein kinase B (PKB) [32–34] or inhibiting glycogen synthase kinase-3 (GSK-3β) [34, 35]. Akt kinase also inhibits apoptosis by phosphorylating GSK-3β [36] and BAD [37], rendering them inactive. Low levels of Akt kinase, high levels of GSK-3β kinase and activated BAD are associated with increased neuronal cell death [38–41]. Activated BAD mediates cell death by disrupting mitochondrial membrane permeability and promoting cytochrome c release, which activate caspases [42, 43]. Perturbations in mitochondrial membrane permeability increase cellular free radicals that cause mitochondrial DNA damage, impair mitochondrial function, and activate pro-apoptosis cascades [44, 45].

Previous studies using in vitro exposure models demonstrated that ethanol profoundly inhibits insulin-stimulated survival and mitochondrial function in neuronal cells [11, 12, 15, 18, 46]. These adverse effects of ethanol were mediated by inhibition of insulin-stimulated tyrosyl phosphorylation of the insulin receptor and IRS-1, and downstream signaling through PI3 kinase [11, 12, 15, 18, 46]. The present studies extend investigations to an in vivo model to determine if similar abnormalities occur following chronic gestational exposure to ethanol, contributing therefore to the neuronal loss and impaired function. The in vivo model was generated by feeding pregnant rats either an ethanol-containing or isocaloric control diet. Cerebellar tissue harvested from postnatal day 2 pups was used to generate short-term neuronal cultures for evaluating the effects of ethanol on insulin-stimulated viability, mitochondrial function, and survival mechanisms. Cerebellar neurons were studied because they represent major in vivo targets of ethanol neurotoxicity.

Materials and methods

In vivo model of chronic ethanol exposure

Long-Evans female rats were adapted to an ethanol-containing or isocaloric control diet (BioServe) over a 3-week interval, after which the rats were mated with normal males. Ethanol comprised 11.8%, 23.6%, and 35.4% of the caloric content of the feedings during the first, second, and third weeks of adaptation. Rats were maintained on the 35.4% ethanol-containing or isocaloric control diet throughout pregnancy. This level of ethanol consumption produces blood concentrations between 50 and 60 mM, comparable to the levels found in sera of chronic alcoholics [47]. The rats were monitored daily to ensure equivalent caloric consumption and maintenance of body weight. Typically, in the ethanol-fed group, the litter sizes were reduced by 20% and pup mean body weight was reduced by 10–15%. Histological sections of cerebellar tissue fixed with Histochoice (Amresco, Solon, Ohio) and embedded in paraffin were stained with Hoechst H33258 and examined by fluorescence microscopy.

Cell culture

Primary neuronal cultures were generated with cerebellar tissue harvested from individual control or ethanol-exposed postnatal (P) day 2 pups [48], and generally between 12 and 24 replicate cultures (pups per group) were used for each study. Cultures were maintained for 24 h in Dulbecco's modified Eagle's medium (DMEM) supplemented with 50 nM insulin (Humulin, Eli Lilly & Co., Indianapolis, Ind.), 2 mM glutamine, 10 mM non-essential amino acid mixture (Gibco-BRL, Grand Island, N. Y.), 25 mM KCl, and 9 g/l glucose. Cells were not exposed to ethanol in vitro. Ultrastructural studies were performed with 24 h cultures to detect ethanol-induced morphological abnormalities. Intact cultures were fixed overnight at 4 °C in 2% glutaraldehyde prepared in buffer containing 50 mM cacodylate, pH 7.4, 2 mM $MgSO_4$, and 0.25 M sucrose. The cells were then postfixed in 1% osmium tetroxide prepared in 50 mM cacodylate, pH 7.4 at 4 °C for 1 h and stained with 1% uranyl acetate overnight. After dehydration in graded ethanol solutions, the cells were collected by gentle scraping and embedded

in Epon resin. Ultrathin sections were examined by transmission electron microscopy using core research facilities at the Rhode Island Hospital.

Viability and mitochondrial assays

Microcultures (96-well plates) in which 5×10^4 viable cells were seeded per well were used for assays of neuronal viability, mitochondrial function, and pro-apoptosis gene expression [15, 49]. The 96-well format permitted simultaneous analysis of 8–24 replicate cultures to generate results for statistical analysis. Cell viability was measured using the crystal violet (CV) assay [11, 49, 50]. Mitochondrial function was assessed using the 3-[4,5-dimethylthiazol-2-yl]-2,5-diphenyltetrazolium bromide (MTT) assay and MitoTracker labeling [51]. CV and MTT absorbances (540 nm) were measured in a Spectracount microplate reader (Packard Instrument Co., Meriden, Conn.). Titration studies demonstrated that CV and MTT absorbances increased linearly with cell density between 10^4 and 5×10^5 cells/well, thus enabling intergroup comparisons of viability and mitochondrial function. All experiments were repeated at least three times.

Cellular labeling with MitoTracker fluorescent mitochondria-specific cell-permeable dyes was used to evaluate mitochondrial function and mitochondrial mass. MitoTracker Red (CM-H_2Xros) accumulates only in metabolically active mitochondria and the reduced dihydrotetramethylrosamine is rendered fluorescent via oxidation within mitochondria. MitoTracker Green FM labels mitochondria irrespective of oxidative activity and is therefore used to assess Mt mass. Cells grown in 96-well plates were incubated with MitoTracker Red or MitoTracker Green FM for 15 min according to the manufacturer's instructions (Molecular Probes, Eugene, Ore.). After rinsing in Tris-buffered saline (TBS; 50 mM Tris, pH 7.5, 0.9% NaC), fluorescence light units (FLU) were measured with a Fluorocount microplate reader (Packard Instrument Company).

To determine if ethanol toxicity was partly due to impaired membrane integrity or oxidative stress, live cultures were incubated with dihydrorosamine-6G (DHR) or Calcein AM for 15–30 min at 37 °C. Calcein AM is a polar dye that is rendered fluorescent by acid hydrolysis and is retained in cells that have good membrane integrity. DHR is a Leuco dye that passively diffuses across cell membranes and is rendered fluorescent upon reaction with hydrogen peroxide or nitric oxide in the presence of cytochrome c, peroxidase or Fe^{2+}. DHR fluorescence therefore indirectly reflects the production of reactive oxygen species. After labeling according to the manufacturerís protocols (Molecular Probes), the cells were rinsed in TBS and fluorescence emission was measured in a Fluorocount plate reader (Packard Instrument Company). Subsequently, the cells were stained with H33258 to determine cell density using the Fluorocount. H33258 FLU increase linearly with cell number between 1×10^4 and 5×10^5 cells per well. MitoTracker Red, MitoTracker Green, Calcein AM, and DHR fluorescence intensities were corrected for differences in cell density. Results from 16–24 replicate culture wells were analyzed statistically.

The microtiter immunocytochemical ELISA assay of protein expression

The MICE assay is a rapid and sensitive method for quantifying immunoreactivity in 96-well cultures [52]. It was used to measure cellular expression of p53, Fas-receptor (CD95), Fas-ligand, Akt, phospho (p)-Akt, GSK-3β, pGSK-3β, BAD, and pBAD. The cultures were fixed in Histochoice (Amresco), permeabilized by a 5-min treatment with 0.05% saponin in TBS, then treated with 0.3% H_2O_2 to quench endogenous peroxidase activity. Nonspecific binding sites were adsorbed with Superblock-TBS (Pierce, Rockford, Ill.). The cells were incubated overnight at 4 °C with primary antibody diluted (0.5–1.0 µg/ml) in TBS containing 0.05% Tween-20 and 0.5% bovine serum albumin (TBST-BSA). Immunoreactivity was detected using horseradish peroxidase-conjugated secondary antibody (Pierce) and either TMB-soluble peroxidase substrate or for increased sensitivity, PicoWest luminescence reagents (Pierce). TMB absorbances were measured at 450 nm using a Spectracount plate reader (Packard Instrument Company). Luminescence was measured in relative light units (RLU) using a TopCount machine (Packard Instrument Company).

Comparing the levels of protein expression required correcting for differences in cell density. After measuring immunoreactivity, the cells were washed in TBS then stained with 0.1% Coomassie blue dye dissolved in 40% methanol/10% acetic acid. After extensive washing with water, the plates were dried and dye was eluted with 200 µl/well of 1% SDS in PBS [52]. Absorbances (560 nm) were measured using a Spectracount plate reader. The MICE index was calculated from the ratio of the absorbances corresponding to immunoreactivity and cell density for each well. Coomassie blue absorbances increase linearly with cell density between 1×10^4 and 5×10^5 cells per well. Eight to 24 replicate culture wells were analyzed in each experiment, and all experiments were repeated at least three times.

Western blot analysis

Cultured cells were lysed in radioimmunoprecipitation assay (RIPA) buffer (50 mM Tris-HCl, pH 7.5, 1% NP-40, 0.25% sodium deoxycholate, 150 mM NaCl, 1 mM EDTA, 2 mM EGTA) containing protease and phosphatase inhibitors (1 mM NaF, 1 mM $Na_4P_2O_7$, 2 mM Na_3VO_4, 1 mM phenylmethylsulfonyl fluoride, 1 µg/ml each of aprotinin, pepstatin A, and leupeptin) [53]. Cellu-

lar debris was pelleted by centrifuging the samples at 14,000 × g for 15 min at 4 °C, and supernatant fractions were used. Protein concentration was measured with the BCA assay (Pierce). Aliquots of 60 or 100 µg protein were used for Western blot analysis ([54]. Immunoreactivity was detected with horseradish peroxidase-conjugated secondary antibody, Supersignal enhanced chemiluminescence reagents (Pierce Chemical Company), and the Kodak Digital Science Imaging Station (NEN Life Sciences Products, Boston, Mass.).

Source of reagents

Monoclonal antibodies to Fas receptor, Fas ligand, p53, and proliferating cell nuclear antigen (PCNA) were purchased from Transduction Laboratories (Lexington, Ken.). Phospho-specific antibodies to Akt, GSK-3β, and BAD, and total protein antibodies to Akt and BAD were obtained from Cell Signaling (Beverly, Mass.). Monoclonal antibodies to glyceraldehyde-3-phosphate dehydrogenase (GAPDH) and GSK-3 were purchased from Chemicon Corp. Fluorescent dyes were obtained from Molecular Probes. All other reagents were purchased from CalBiochem (San Diego, Calif.) or Sigma-Aldrich (St. Louis, Mo.).

Statistical analysis

Data depicted in the graphs represent the mean ± SD of results obtained with cerebellar cultures generated from 12–24 individual control or ethanol-exposed postnatal (P) day 2. All experiments were repeated at least three times and representative results are shown. Inter-group comparisons were made with Student t-tests using the Number Cruncher Statistical Systems (Dr. Jerry L. Hintze, Kaysville, Utah).

Results

Ethanol-induced cerebellar hypoplasia

Chronic gestational exposure to ethanol in rats produced cerebellar hypoplasia, which is characteristic of FAS [1]. There were no overt ethanol-associated behavioral disturbances detected, perhaps because on postnatal day 2 when the pups were sacrificed to generate neuronal cultures, the cerebella were immature even in control animals. Paraffin-embedded histological sections of brain harvested from P2 pups ($n = 12$ for each group) were stained with Hoechst H33258 and examined by fluorescence microscopy. The cerebella of ethanol-exposed pups exhibited hypoplasia with poorly developed folia, impaired neuronal migration, and increased apoptosis (fig. 1), as reported previously in experimental models of FAS [3–7]. Apoptotic nuclei, characterized by their condensed, bright fluorescence, were widely distributed in cerebellar tissue of ethanol-exposed rats.

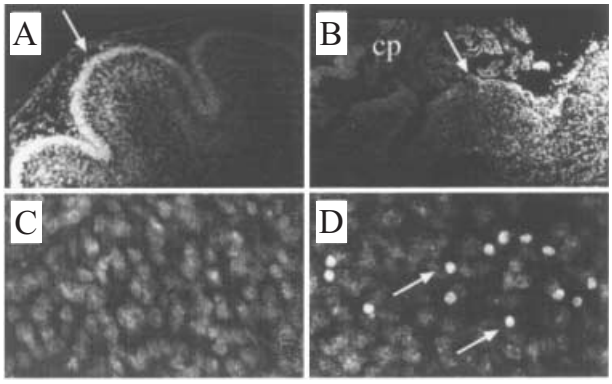

Figure 1. Ethanol-induced cerebellar abnormalities. Pregnant rats were fed with a 35.4% ethanol-containing or isocaloric control liquid diet. Cerebella harvested from postnatal day 2 pups were fixed in Histochoice and embedded in paraffin. Histological sections were stained with propidium iodide and examined by fluorescence microscopy. Shown are control cerebellar cortex with well-developed folia and lamination (*A*), and uniform labeling of nuclei (*C*); ethanol-exposed cerebellar cortex with simplified folia, poor lamination (*B*), and numerous cells with condensed, pyknotic nuclei characteristic of apoptosis (arrows) (*D*) (cp, choroids plexus). Original magnifications: *A*, *B* × 60; *C*, *D* × 500.

Gestational exposure to ethanol impairs insulin-stimulated neuronal viability

Previous studies demonstrated that in vitro exposure to ethanol impairs insulin stimulated neuronal viability and mitochondrial function [11, 12, 15]. The present studies determined if similar abnormalities in insulin responsiveness occurred with chronic gestational exposure to ethanol. Neuronal cultures generated from P2 control or ethanol-exposed rat pup cerebella were stimulated with 50 nM insulin for 24 h without further ethanol treatment. CV assays detected significantly lower mean cell densities ($p < 0.001$; fig. 2A) in cultures generated from ethanol-exposed relative to control pups.

Chronic gestational exposure to ethanol adversely affects mitochondria

Using the MTT assay, we detected significantly reduced levels of insulin-stimulated mitochondrial function in cultures generated from ethanol-exposed relative to control pups ($p < 0.001$; fig. 2B). To determine if the inhibition of mitochondrial enzyme activity was caused by impaired function or reductions in mitochondrial mass (abundance), cultures were labeled with MitoTracker dyes that are rendered fluorescent after localizing within mitochondria. MitoTracker FLU values were corrected for differences in cell density using H33258 labeling indices. The insulin-stimulated, ethanol-exposed cultures had significantly reduced levels of MitoTracker Red ($p < 0.001$) and MitoTracker Green ($p < 0.05$) fluorescence relative to control cultures (fig. 3). Corresponding with results obtained by in vitro

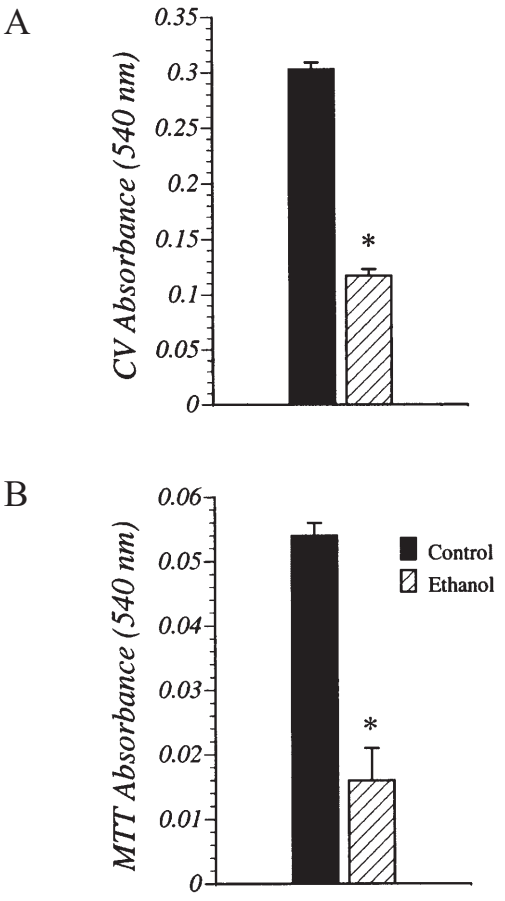

Figure 2. Ethanol-impaired, insulin-stimulated neuronal viability and mitochondrial function in cerebellar cultures. Female rats were fed with 34% ethanol-containing or isocaloric control liquid diets throughout pregnancy. Cerebellar neurons isolated from postnatal day 2 pups were seeded into 96-well plates (5×10^4 cells/well) and cultured for 24 h in DMEM containing 25 mM KCl and 50 nM insulin. Cell viability was measured in 24 replicate culture wells using the crystal violet (CV) assay (*A*), and mitochondrial function was measured with the MTT assay (*B*). Graphs depict the mean ± SD of CV or MTT absorbances at 540 nm. Between-group comparisons were made using Student t-tests (* $p < 0.001$).

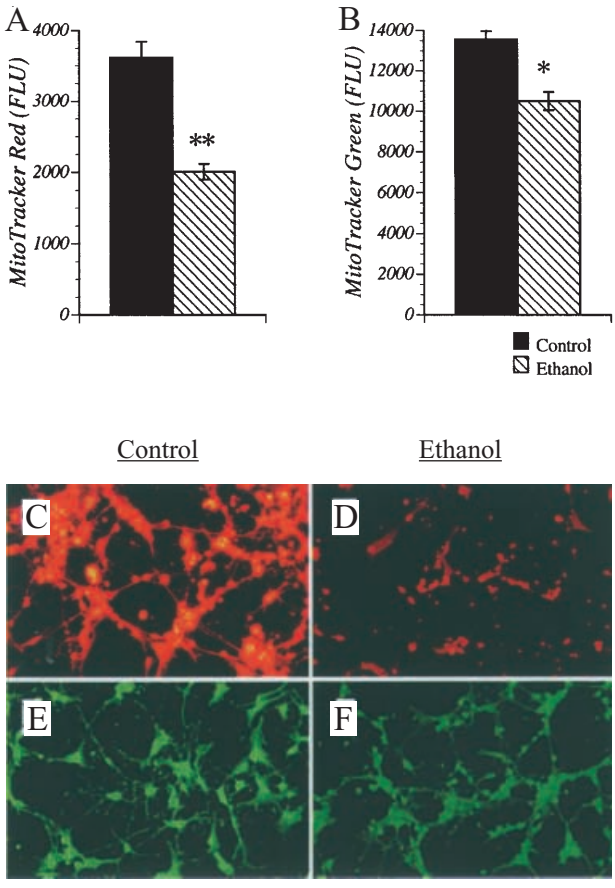

Figure 3. Ethanol-impaired mitochondrial function. Cerebellar neuron cultures generated from ethanol-exposed and control pups were stimulated with insulin (50 nM) for 24 h and evaluated for mitochondrial function or mitochondrial mass by labeling with MitoTracker Red or MitoTracker Green fluorescent dyes. Fluorescence intensity was measured (fluorescence light units; FLU) with a Fluorocount machine. The graphs depict the mean ± SD of MitoTracker Red FLU (*A*) and MitoTracker Green FLU (*B*) in 24 replicate cultures. Graphed data display results corrected for differences in cell density using H33258 FLU indices. Statistical comparisons were made using Student t-tests (** $p < 0.001$; * $p < 0.05$). Fluorescence microscopy was performed to visualize MitoTracker labeling in control (*C*, *E*) and ethanol-exposed (*D*, *F*) cultures. MitoTracker Red (*C*, *D*) and (*E*, *F*) fluorescence labeling. Representative field areas are shown.

ethanol treatment of neuronal cells [11, 12, 15], gestational exposure to ethanol caused proportionally greater reductions in MitoTracker Red than MitoTracker Green fluorescence. Fluorescence microscopic studies confirmed the ethanol-induced reductions in insulin-stimulated MitoTracker Red and MitoTracker Green labeling, and also showed the greater inhibitory effect on MitoTracker Red compared to MitoTracker Green fluorescence (fig. 3C–F). Electron microscope studies demonstrated that the ethanol-induced abnormalities in mitochondrial function were associated with increased densities of swollen, irregular mitochondria, cytoplasmic vacuolations, and electron-dense accumulations within mitochondria (fig. 4) as described in other models of chronic ethanol exposure [55, 56].

Adverse effects of ethanol on membrane integrity and oxidant production

Previous in vitro experiments demonstrated that ethanol inhibition of insulin-stimulated mitochondrial function was associated with reduced membrane integrity and increased generation of reactive oxygen species [12, 15]. To determine if the same abnormalities occur following chronic gestational exposure to ethanol, insulin-stimulated cultures were evaluated for Calcein AM retention and DHR fluorescence, as measures of membrane permeability and oxidative stress, respectively. Calcein AM and DHR fluorescence levels were corrected for cell

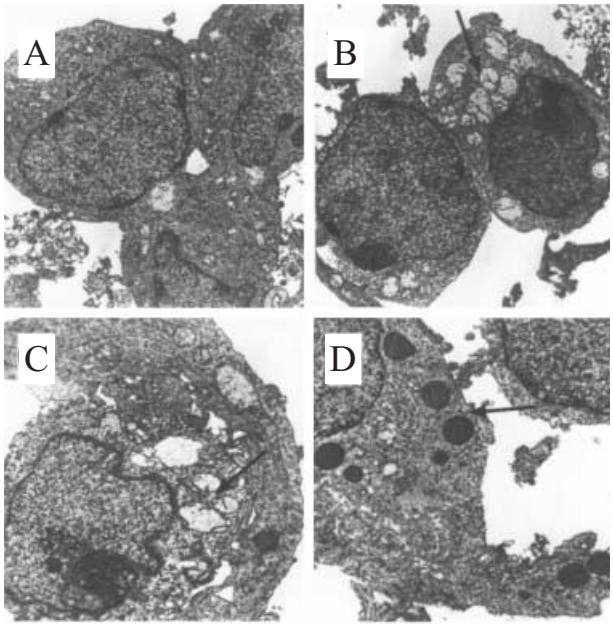

Figure 4. Ultrastructural studies of insulin-stimulated control (*A*) and ethanol-exposed (*B–D*) cerebellar cultures. (*A*) Neuronal cells in control cultures had relatively uniform nuclear morphology and mainly normal mitochondria, although occasional mitochondria exhibited swelling or vacuolation. (*B–D*) Neuronal cells in cultures generated from ethanol-exposed pups exhibited irregular nuclear morphology, prominent swelling and vacuolation of mitochondria (*B*, *C*; arrows), and electron-dense alterations of mitochondria (*D*; arrow).

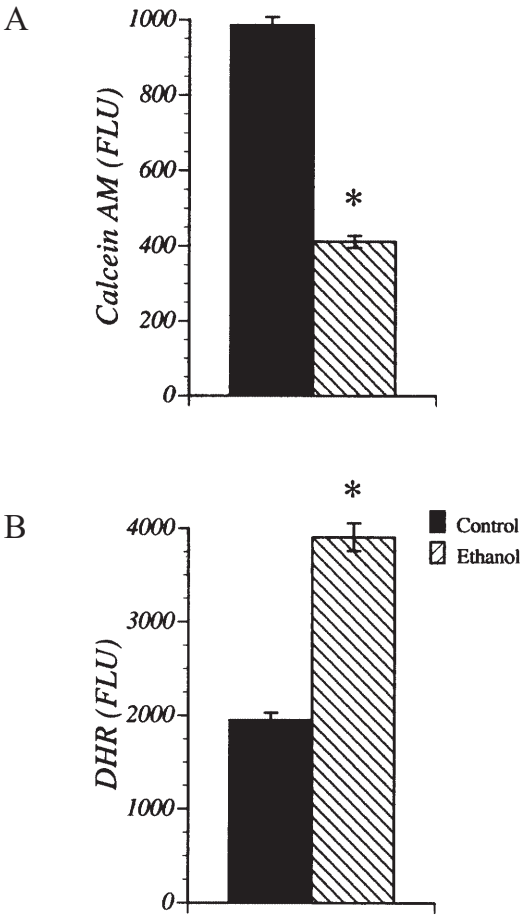

Figure 5. Chronic gestational exposure to ethanol increases membrane permeability and oxidative stress. Cerebellar neuron cultures generated from control and ethanol-exposed pups were stimulated with insulin (50 nM) for 24 h and evaluated for Calcein AM retention and dihydrorosamine (DHR) fluorescence as indices of membrane integrity and oxidant production, respectively. Live cells were labeled for 15 min at 37 °C with fluorescent dyes. Fluorescence intensity FLU was measured using a Fluorocount machine. The graphs depict the mean ± SD of Calcein AM FLU (*A*) and DHR FLU (*B*) in 24 replicate cultures. Graphed data display results corrected for differences in cell density using H33258 FLU indices. Statistical comparisons were made using Student t-tests (* $p < 0.001$).

density using H33258 FLU indices. As illustrated in figure 5, cultures generated from ethanol-exposed pups had significantly reduced levels of Calcein AM retention and increased DHR fluorescence relative to controls (both $p < 0.001$). These findings suggest that chronic gestational exposure to ethanol impairs membrane integrity and increases oxidative stress in immature CNS neurons.

Effects of ethanol on proteins that regulate neuronal viability and function

In vitro exposure studies suggested that ethanol impairment of insulin-stimulated survival and mitochondrial function was mediated by activation of pro-apoptosis mechanisms [11, 12]. Correspondingly, neuronal cultures generated from ethanol-exposed pups had significantly higher levels of p53, Fas receptor (Fas-R), and Fas ligand (Fas-L) expression relative to control cultures (all $p < 0.01$; fig. 6). In contrast, expression of GAPDH, an important insulin-responsive gene [57] that regulates energy metabolism, was inhibited by in utero ethanol exposure ($p < 0.001$), and PCNA, a marker of cell growth, was similarly expressed in neuronal cultures generated from control or ethanol-exposed pups (fig. 6).

Effects of ethanol on signaling mechanisms that regulate neuronal viability and function

Insulin-stimulated levels of Akt and p-Akt, p-GSK-3β, GSK-3, BAD, and p-BAD were measured using a luminescence-based MICE assay. To confirm the results of the MICE assay, GSK-3β and Akt phosphorylation were examined by Western blot analysis using the same antibodies as for the MICE assay. In short-term stimulation studies in which growth factor-deprived (12 h) cultures were exposed to 50 nM insulin for 0–30 min, p-Akt levels increased sharply in control cultures, reaching peak levels within 5 min (fig. 7A). In cultures generated from ethanol-exposed pups, p-Akt expression increased

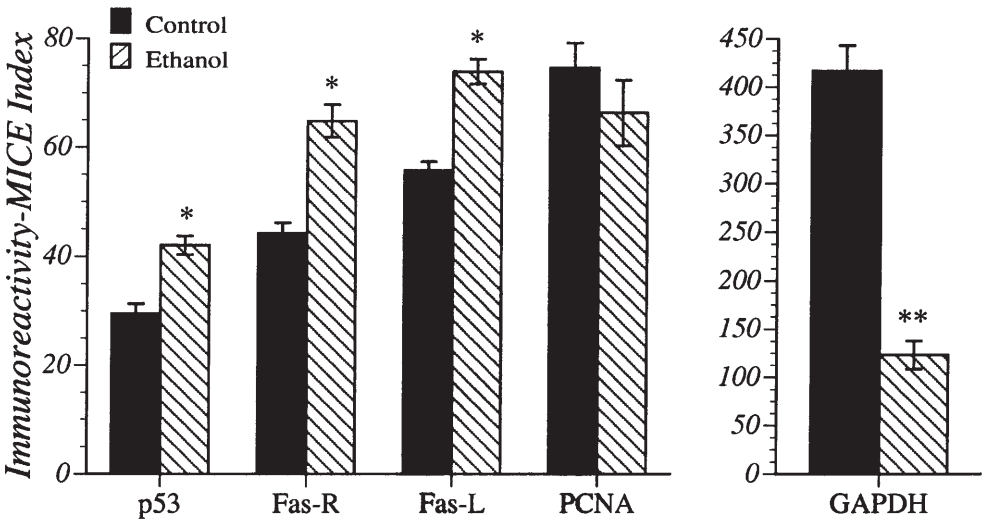

Figure 6. Chronic gestational exposure to ethanol increases pro-apoptosis gene expression and inhibits insulin-responsive gene expression. Cerebellar neuron cultures generated from control and ethanol-exposed pups were stimulated with insulin (50 nM) for 24 h and evaluated for p53, Fas receptor (Fas-R), Fas ligand (Fas-L), PCNA, and GAPDH expression using the microtiter immunocytochemical ELISA (MICE) assay (see Materials and methods). Immunoreactivity was adjusted for differences in cell density and net levels of immunoreactivity are reflected by the MICE indices. The graphs depict mean ± SD of protein levels measured in 24 replicate cultures. Statistical comparisons were made using Student t-tests (* $p < 0.01$; ** $p < 0.001$).

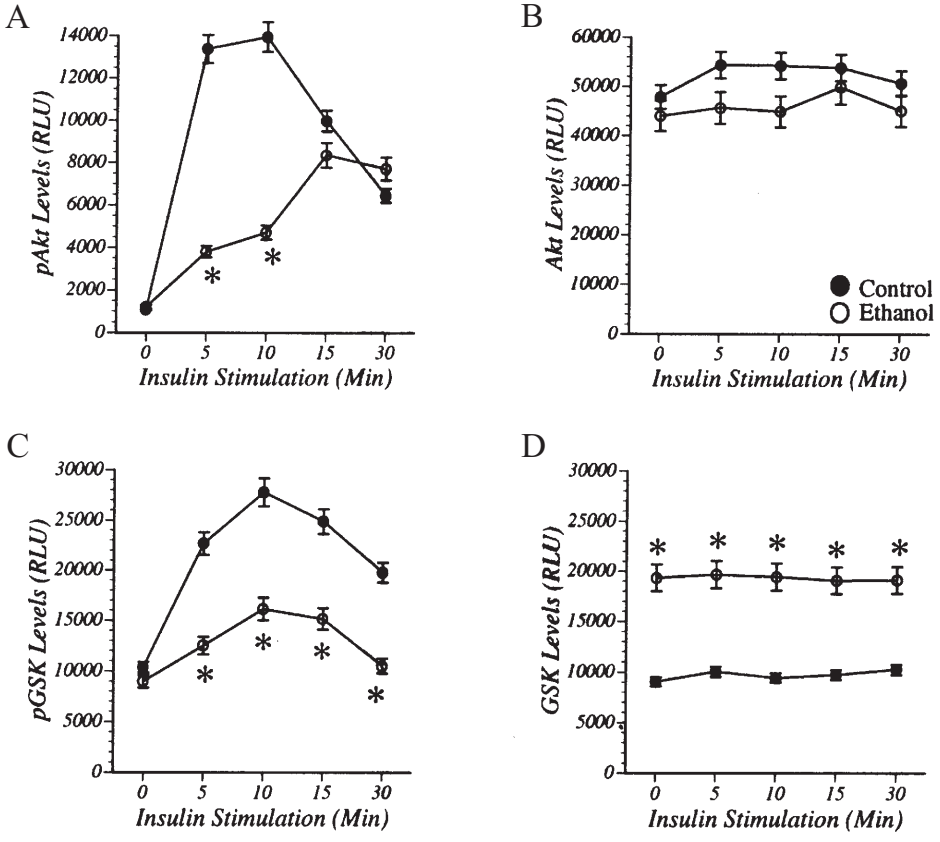

Figure 7. Gestational exposure to ethanol inhibits insulin-stimulated phosphorylation of Akt and GSK-3β. Cerebellar neuron cultures generated from ethanol-exposed and control pups were stimulated with insulin (50 nM) for 0–30 min after a 12-h period of growth factor deprivation. Immunoreactivity to phospho (p)Akt, Akt, pGSK-3β, and GSK-3 was measured by the MICE assay with luminescence detection quantified in a TopCount machine. The graphs depict mean ± SD of protein levels quantified in 16 replicate cultures (* $p < 0.001$).

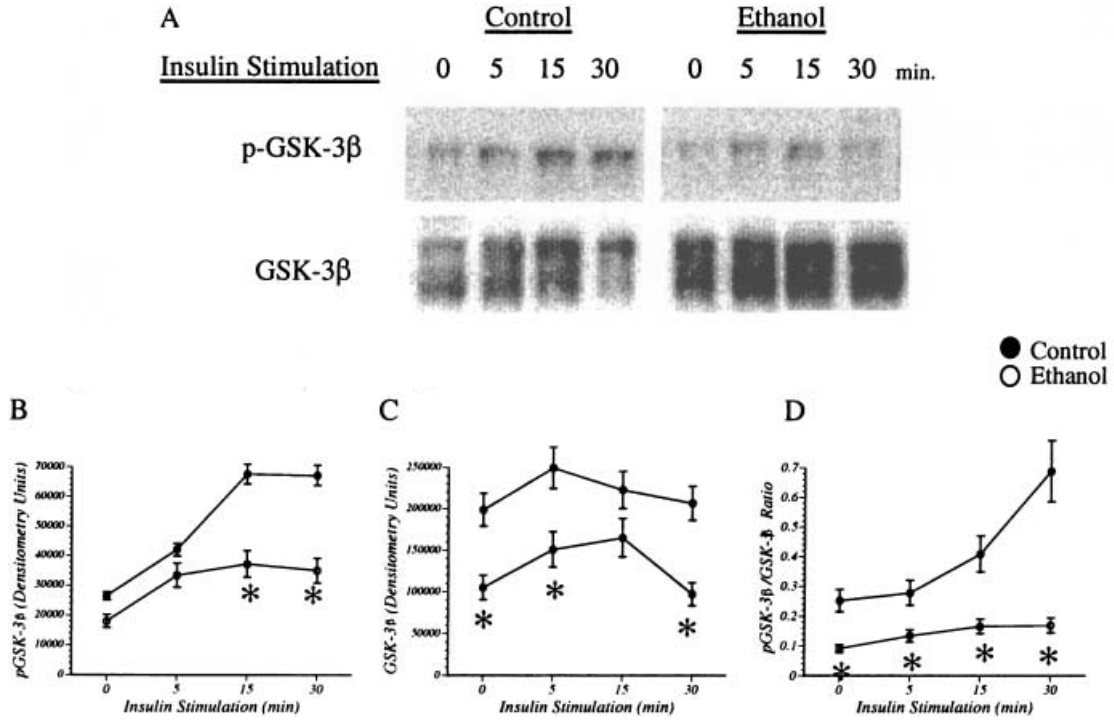

Figure 8. Gestational exposure to ethanol impairs insulin-stimulated phosphorylation of GSK-3β. Cerebellar neuron cultures generated from ethanol-exposed and control pups were stimulated with insulin (50 nM) for 0–30 min after a 12-h period of growth factor deprivation. Cells were lysed in RIPA buffer and samples containing equivalent amounts of protein were subjected to Western blot analysis to detect phospho (p)GSK-3β or total GSK-3 protein. Representative Western immunoblotting results are shown in Panel *A*. GSK-3 protein was detected as a ~ 46 to 51-kDa doublet corresponding to the α (upper band) and β (lower band) subunits, whereas phospho-GSK-3β was detected as a single band. Levels of immunoreactivity were measured with the Kodak Digital Image Station, and the results (mean ± SD) from three replicate experiments are depicted in the graphs. Statistical comparisons were made using ANOVA (* $p < 0.005$). Antibodies used for these experiments were the same as those employed for the MICE assay shown in fgure 7. (*B*) Insulin-stimulated phosphorylation of GSK-3β. (*C*) Levels of total GSK-3 protein detected in the same samples used to detect pGSK-3β. (*D*) The pGSK-3β/GSK-3 ratios after 0, 5, 15, or 30 min of insulin stimulation.

more gradually in response to insulin stimulation, and peak levels were detected after 15 min. Chronic gestational exposure to ethanol delayed the time course and reduced the peak levels of p-Akt. In contrast, Akt protein expression was similar and not modulated by insulin in control and ethanol-exposed cultures (fig. 7B). Western blot analysis detected the expected ~ 60-kDa proteins with both anti-Akt and anti-phospho-Akt, and confirmed the inhibitory effects of ethanol on insulin-stimulated Akt phosphorylation demonstrated in figure 7 using the MICE assay (data not shown).

Cultures generated from ethanol-exposed pups also had reduced levels of GSK-3β phosphorylation, and increased levels of GSK-3 protein relative to control (fig. 7C, D). In control cultures, insulin-stimulated phosphorylation of GSK-3β increased sharply and peaked at the 10-min time point, after which the levels declined. The ethanol-exposed cultures had a similar time course of insulin-stimulated GSK-3β phosphorylation, but the peak levels were nearly 50% lower than in control cultures (fig. 7C). Although GSK-3 protein expression was not modulated by short-term insulin stimulation, the levels were approximately twofold higher in ethanol-exposed relative to control cultures (fig. 7D). These effects of gestational exposure to ethanol on GSK-3 expression and GSK-3β phosphorylation were confirmed by Western blot analysis. As shown in figure 8, the antibody to GSK-3 detected two distinct bands at ~ 46- to 51-kDa, corresponding to GSK-3α (upper) and GSK-3β (lower). The Western blot studies also demonstrated significantly higher levels of insulin-stimulated phospho-GSK-3β, and lower levels of total GSK-3 protein in neuronal cultures generated from control cerebella compared with those generated from ethanol-exposed cerebella (fig. 8A–C; $p < 0.005$), corresponding with results of the MICE assay. The slight modulations in the levels of GSK-3 protein observed with insulin stimulation were not statistically significant, but most likely reflected the detection of both phospho-GSK-3β and total GSK-3 protein. The inhibitory effect of ethanol on insulin-stimulated GSK-3β phosphorylation was best revealed with graphs depicting the calculated p-GSK-3β/GSK-3 ratios (fig. 8D). The curve for control cultures showed progressively increased p-GSK-3β/GSK-3 levels over the 30-min period of study,

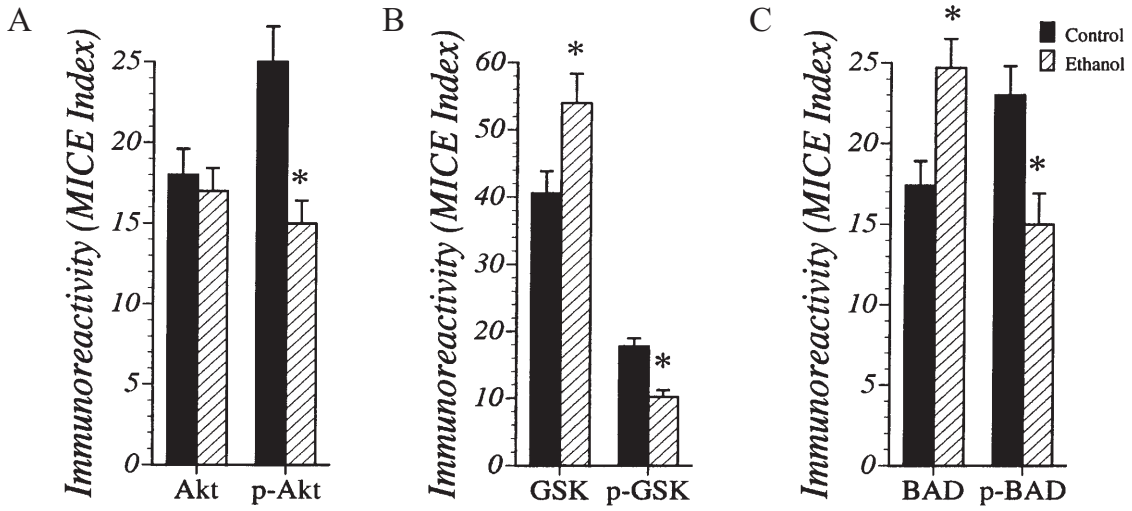

Figure 9. Ethanol inhibits insulin-stimulated survival signaling in cerebellar neurons. Cerebellar neuron cultures generated from ethanol-exposed and control pups were stimulated with insulin (50 nM) for 24 h and evaluated for Akt, phospho (p) Akt, GSK-3, p-GSK-3β, BAD, and p-BAD using the MICE assay (see Material and methods). Immunoreactivity was adjusted for differences in cell density and net levels of immunoreactivity are reflected by the MICE indices. The graphs depict mean ± SD of protein levels measured in 24 replicate cultures. Intergroup statistical comparisons were made using Student t-tests (* $p < 0.01$).

whereas the curve corresponding to ethanol-exposed cerebellar cultures was relatively flat.

The MICE assay (TMB-substrate based) was used to measure Akt, p-Akt, GSK-3, p-GSK-3β, BAD, and p-BAD expression in cultures that had been stimulated with insulin for 24 h. These studies demonstrated significantly reduced levels of p-Akt ($p < 0.001$), p-GSK-3β, and p-BAD ($p < 0.01$), and significantly increased levels of total GSK-3 and total BAD protein ($p < 0.01$) in cultures generated from ethanol-exposed rat pup cerebella (fig. 9). Therefore, observations with short-term stimulation assays were similar to the long-term responses to insulin.

Discussion

Previous studies demonstrated that in vitro exposure to ethanol impairs insulin-stimulated neuronal viability [11, 12, 15, 46]. This adverse effect of ethanol on neuronal survival was associated with reduced levels of insulin-stimulated tyrosyl phosphorylation of the insulin receptor and IRS-1, and impaired signaling through PI3 kinase [11, 12, 15, 18, 46]. To determine the biological relevance of these findings, we extended our investigations to an in vivo model produced by feeding pregnant rats an ethanol-containing or isocaloric control liquid diet throughout gestation. The cerebella of ethanol-exposed pups were hypoplastic and exhibited evidence of impaired cellular migration. In addition, the associated high densities of propidium iodide-labeled pyknotic nuclei suggested that the ethanol-induced cerebellar hypoplasia was mediated at least in part by apoptosis. Our study demonstrates that chronic gestational exposure to ethanol impairs insulin-stimulated neuronal viability and mitochondrial function. In a study published by Ikonomidou et al. [13], the authors showed that neuronal loss following acute postnatal exposure to high concentrations of ethanol could be mediated by inhibition of NMDA glutamate receptor function. Therefore, the mechanisms of neuronal loss associated with these two models differ substantially. However, this discrepancy could be explained due to the marked differences in duration, time course, and developmental age of the animals at the time of ethanol exposure.

Insulin-stimulated survival functions were examined in cerebellar neuron cultures generated from postnatal day 2 pups. However, to independently assess the integrity of insulin signaling mechanisms, we measured expression levels of GAPDH protein, which is encoded by an insulin-responsive gene and therefore downstream in the cascade [57]. Using the MICE assay, we detected substantially reduced GAPDH expression in cultures generated from ethanol-exposed pups, thus confirming that chronic gestational exposure to ethanol inhibits insulin-signaling mechanisms in CNS neurons. The significantly reduced levels of insulin-stimulated neuronal viability observed in cultures generated from ethanol-exposed pups corresponds with results previously obtained with in vitro exposure models [11, 12, 15, 18, 46]. The associated increased levels of p53, Fas-R, and Fas-L expression suggest that the impaired neuronal viability was mediated in part by activation of pro-apoptosis mechanisms. In contrast, we detected no significant adverse effects of ethanol on insulin-stimulated PCNA expression, consistent with previous observation [11, 18].

In the present study, we also observed significantly reduced levels of insulin-stimulated mitochondrial function in neuronal cultures generated from ethanol-exposed cerebella, corresponding with results obtained previously using in vitro exposure models [12, 15]. Mitochondrial function was measured by two independent methods: the MTT assay and MitoTracker Red labeling. MTT activity reflects conversion of MTT dye to a purple formazen precipitate by mitochondrial reductase [51], whereas MitoTracker Red accumulates in metabolically active mitochondria and the reduced dihydrotetramethylrosamine is rendered fluorescent following oxidation within mitochondria. One difference between the effects of in vivo and in vitro ethanol exposure is that the former resulted in significantly reduced MitoTracker Green fluorescence, indicating a loss of mitochondrial mass/abundance. However, the relative reduction in mitochondrial function was greater than the decrease in mitochondrial mass. Impaired mitochondrial function was associated with ultrastructural abnormalities characterized by swelling, vacuolation, or accumulation of electron-dense material in neuronal mitochondria in insulin-stimulated cultures generated from ethanol-exposed rat pup cerebella, corresponding with previously reported findings in ethanol-exposed experimental animals [55, 56]. Together, these results provide evidence that chronic gestational exposure to ethanol impairs insulin-stimulated mitochondrial function in CNS neurons. Persistence of ethanol-induced mitochondrial abnormalities during the early postnatal period could adversely affect further brain development.

The mechanisms by which ethanol may impair mitochondrial function are complex but likely linked to mitochondrial DNA damage. In this regard, Ramachandran et al. [16] detected increased mitochondrial DNA damage and mitochondrial permeability transition in rat brains following chronic gestational exposure to ethanol. Using in vitro exposure models, we also detected ethanol-induced mitochondrial DNA damage in CNS-derived neuronal cells [12], and demonstrated greater impairments in mitochondrial function with insulin as opposed to other types of growth factor stimulation, e.g. nerve growth factor [11, 12]. These results suggest that insulin-stimulated viability and mitochondrial function may represent particularly vulnerable targets of ethanol neurotoxicity in immature neuronal cells.

Previous experiments demonstrated that in vitro ethanol exposure impaired cell membrane integrity and increased the generation of reactive oxygen species in neuronal cells [12, 15]. To determine if the same abnormalities occurred in vivo, insulin-stimulated cultures were evaluated for Calcein AM retention and DHR fluorescence as measures of membrane permeability and oxidative stress, respectively. Those studies demonstrated that cultures generated from ethanol-exposed pups had significantly reduced levels of Calcein AM retention and increased DHR fluorescence. Consequences of impaired neuronal membrane integrity include increased calcium influx and excitotoxic injury. Potential mechanisms of ethanol-impaired membrane integrity and oxidant production include mitochondrial dysfunction, membrane lipid peroxidation, and mitochondrial DNA damage [12, 15, 16].

Using in vitro exposure models, we previously demonstrated that ethanol impairments of insulin-stimulated survival and mitochondrial function were associated with activation of pro-apoptosis mechanisms [11, 12]. Similarly, in other models of neuronal injury or neurodegeneration, neuronal apoptosis was mechanistically linked to increased expression of pro-apoptosis genes or inhibition of survival genes [50, 58, 59]. Correspondingly, in neuronal cultures generated from ethanol-exposed pups, the levels of p53, Fas receptor, and Fas ligand expression were significantly increased relative to control. These effects of ethanol may have been mediated by oxidative stress induced by the inhibition of insulin-stimulated survival signaling.

PI3 kinase is an important mediator of neuronal survival. PI3 kinase mediates survival by phosphorylating Akt and activating Akt kinase [32, 34, 60], or by phosphorylating GSK-3β and inhibiting its activity [34, 35]. Akt kinase functions by phosphorylating GSK-3β and BAD, which are pro-apoptotic [34, 37, 40, 43], and rendering them inactive. Our studies focused on measuring insulin-stimulated Akt, GSK-3β, and BAD phosphorylation to assess survival mechanisms downstream of PI3 kinase. We observed that chronic gestational exposure to ethanol inhibits insulin-stimulated Akt, GSK-3β, and BAD phosphorylation, and also results in increased levels of activated GSK-3β and BAD. The aggregate results suggest that insulin-stimulated CNS neuronal survival mechanisms are impaired by chronic gestational exposure to ethanol, and that the adverse effects of ethanol on insulin signaling in the brain may contribute substantially to neurodevelopmental abnormalities. The administration of insulin sensitizer drugs that optimize insulin signaling [61, 62] may help to improve survival and preserve mitochondrial function in ethanol-exposed developing CNS neurons.

Acknowledgements. This work was supported by grants AA-02666, AA02169 and AA-11431 from the National Institutes of Health.

1 Clarren S. K., Alvord E. J., Sumi S. M., Streissguth A. P. and Smith D. W. (1978) Brain malformations related to prenatal exposure to ethanol. J. Pediatr. **92:** 64–67

2 Liesi P. (1997) Ethanol-exposed central neurons fail to migrate and undergo apoptosis. J. Neurosci. Res. **48:** 439–448

3 Maier S. E., Miller J. A., Blackwell J. M. and West J. R. (1999) Fetal alcohol exposure and temporal vulnerability: regional differences in cell loss as a function of the timing of binge-like alcohol exposure during brain development. Alcohol Clin. Exp. Res. **23:** 726–734

4 Mihalick S. M., Crandall J. E., Langlois J. C., Krienke J. D. and Dube W. V. (2001) Prenatal ethanol exposure, generalized learning impairment, and medial prefrontal cortical deficits in rats. Neurotoxicol. Teratol. **23:** 453–462

5 Miller M. (1992) Effects of prenatal exposure to ethanol on cell proliferation and neuronal migration. In: Development of the Central Nervous System: Effects of Alcohol and Opiates, pp. 47–69, Miller M. W. (ed.), New York, Wiley-Liss

6 Minana R., Climent E., Barettino D., Segui J. M., Renau-Piqueras J. and Guerri C. (2000) Alcohol exposure alters the expression pattern of neural cell adhesion molecules during brain development. J. Neurochem. **75:** 954–964

7 Olney J. W., Ishimaru M. J., Bittigau P. and Ikonomidou C. (2000) Ethanol-induced apoptotic neurodegeneration in the developing brain. Apoptosis **5:** 515–521

8 Yanni P. A. and Lindsley T. A. (2000) Ethanol inhibits development of dendrites and synapses in rat hippocampal pyramidal neuron cultures. Brain Res. Dev. Brain Res. **120:** 233–243

9 Maier S. E., Cramer J. A., West J. R. and Sohrabji F. (1999) Alcohol exposure during the first two trimesters equivalent alters granule cell number and neurotrophin expression in the developing rat olfactory bulb. J. Neurobiol. **41:** 414–423

10 Maier S. E. and West J. R. (2001) Regional differences in cell loss associated with binge-like alcohol exposure during the first two trimesters equivalent in the rat. Alcohol **23:** 49–57

11 Monte S. M. de la, Ganju N., Banerjee K., Brown N. V., Luong T. and Wands J. R. (2001) Partial rescue of ethanol-induced neuronal apoptosis by growth factor activation of phosphoinositol-3-kinase. Alcohol Clin. Exp. Res. **24:** 716–726

12 Monte S. M. de la and Wands J. R. (2001) Mitochondrial DNA damage and impaired mitochondrial function contribute to apoptosis of insulin-stimulated ethanol-exposed neuronal cells. Alcohol Clin. Exp. Res. **25:** 898–906

13 Ikonomidou C., Bittigau P., Ishimaru M. J., Wozniak D. F., Koch C., Genz K. et al. (2000) Ethanol-induced apoptotic neurodegeneration and fetal alcohol syndrome. Science **287:** 1056–1060

14 Zhang F. X., Rubin R. and Rooney T. A. (1998) Ethanol induces apoptosis in cerebellar granule neurons by inhibiting insulin-like growth factor 1 signaling. J. Neurochem. **71:** 196–204

15 Monte S. M. de la, Neely T. R., Cannon J. and Wands J. R. (2001) Ethanol impairs insulin-stimulated mitochondrial function in cerebellar granule neurons. Cell. Mol. Life Sci. **58:** 1950–1960

16 Ramachandran V., Perez A., Chen J., Senthil D., Schenker S. and Henderson G. I. (2001) In utero ethanol exposure causes mitochondrial dysfunction, which can result in apoptotic cell death in fetal brain: a potential role for 4-hydroxynonenal. Alcohol Clin. Exp. Res. **25:** 862–871

17 Seiler A. E, Ross B. N. and Rubin R. (2001) Inhibition of insulin-like growth factor-1 receptor and IRS-2 signaling by ethanol in SH-SY5Y neuroblastoma cells. J. Neurochem. **76:** 573–581

18 Xu Y. Y., Bhavani K., Wands J. R. and Monte S. M. de la (1995) Ethanol inhibits insulin receptor substrate-1 tyrosine phosphorylation and insulin-stimulated neuronal thread protein gene expression. Biochem. J. **310:** 125–132

19 Goodyer C. G, De S. L, Lai W. H, Guyda H. J. and Posner B. I. (1984) Characterization of insulin-like growth factor receptors in rat anterior pituitary, hypothalamus, and brain. Endocrinology **114:** 1187–1195

20 Heidenreich K. A, Vellis G. de and Gilmore P. R. (1988) Functional properties of the subtype of insulin receptor found on neurons. J. Neurochem. **51:** 878–887

21 Hill J. M., Lesniak M. A., Pert C. B. and Roth J. (1986) Autoradiographic localization of insulin receptors in rat brain: prominence in olfactory and limbic areas. Neuroscience **17:** 1127–1138

22 Heidenreich K. A. and Toledo S. P. (1989) Insulin receptors mediate growth effects in cultured fetal neurons. I. Rapid stimulation of protein synthesis. Endocrinology **125:** 1451–1457

23 Pahlman S., Meyerson G., Lindgren E., Schalling M. and Johansson I. (1991) Insulin-like growth factor I shifts from promoting cell division to potentiating maturation during neuronal differentiation. Proc. Natl. Acad. Sci. USA **88:** 9994–9998

24 Xu Y. Y, Bhavani K., Wands J. R. and Monte S. M. de la (1995) Insulin-induced differentiation and modulation of neuronal thread protein expression in primitive neuroectodermal tumor cells is linked to phosphorylation of insulin receptor substrate-1. J. Mol. Neurosci. **6:** 91–108

25 Ullrich A., Bell J. R., Chen E. Y., Herrera R., Petruzzelli L. M., Dull T. J. et al. (1985) Human insulin receptor and its relationship to the tyrosine kinase family of oncogenes. Nature **313:** 756–761

26 O'Hare T. and Pilch P. F. (1990) Intrinsic kinase activity of the insulin receptor. Int. J. Biochem. **22:** 315–324

27 Myers M. G., Sun X. J. and White M. F. (1994) The IRS-1 signaling system. Trends Biochem. Sci. **19:** 289–293

28 Shpakov A. O. and Pertseva M. N. (2000) Structural and functional characterization of insulin receptor substrate proteins and the molecular mechanisms of their interaction with insulin superfamily tyrosine kinase receptors and effector proteins. Membr. Cell Biol. **13:** 455–484

29 Sun X. J., Rothenberg P., Kahn C. R., Backer J. M., Araki E., Wilden P. A. et al. (1991) Structure of the insulin receptor substrate IRS-1 defines a unique signal transduction protein. Nature **352:** 73–77

30 Backer J. M., Myers M. J., Shoelson S. E., Chin D. J., Sun X. J., Miralpeix M. et al. (1992) Phosphatidylinositol 3′-kinase is activated by association with IRS-1 during insulin stimulation. EMBO J **11:** 3469–3479

31 Myers M. G., Backer J. M., Sun X. J, Shoelson S., Hu P., Schlessinger J. et al. (1992) IRS-1 activates phosphatidylinositol 3′-kinase by associating with src homology 2 domains of p85. Proc. Natl. Acad. Sci. USA **89:** 10350–10354

32 Burgering B. M. and Coffer P. J. (1995) Protein kinase B (c-Akt) in phosphatidylinositol-3-OH kinase signal transduction. Nature **376:** 599–602

33 Kulik G., Klippel A. and Weber M. J. (1997) Antiapoptotic signalling by the insulin-like growth factor I receptor, phosphatidylinositol 3-kinase, and Akt. Mol. Cell. Biol. **17:** 1595–1606

34 Pap M. and Cooper G. M. (1998) Role of glycogen synthase kinase-3 in the phosphatidylinositol 3-Kinase/Akt cell survival pathway. J. Biol. Chem. **273:** 19929–19932

35 Delcommenne M., Tan C., Gray V., Rue L., Woodgett J. and Dedhar S. (1998) Phosphoinositide-3-OH kinase-dependent regulation of glycogen synthase kinase 3 and protein kinase B/AKT by the integrin-linked kinase. Proc. Natl. Acad. Sci. USA **95:** 11211–11216

36 Weeren P. C. van, Bruyn K. M. de, Vries-Smits A. M. de, Lint J. van and Burgering B. M. (1998) Essential role for protein kinase B (PKB) in insulin-induced glycogen synthase kinase 3 inactivation. Characterization of dominant-negative mutant of PKB. J. Biol. Chem. **273:** 13150–13156

37 Datta S. R., Dudek H., Tao X., Masters S., Fu H., Gotoh Y. et al. (1997) Akt phosphorylation of BAD couples survival signals to the cell-intrinsic death machinery. Cell 91: 231–241

38 Dudek H., Datta S. R., Franke T. F, Birnbaum M. J., Yao R., Cooper G. M. et al. (1997) Regulation of neuronal survival by the serine-threonine protein kinase Akt. Science **275:** 661–665

39 Eves E. M., Xiong W., Bellacosa A., Kennedy S. G., Tsichlis PN, Rosner M. R. et al. (1998) Akt, a target of phosphatidylinositol 3-kinase, inhibits apoptosis in a differentiating neuronal cell line. Mol. Cell. Biol. **18:** 2143–2152

40 Hetman M., Cavanaugh J. E., Kimelman D. and Xia Z. (2000) Role of glycogen synthase kinase-3beta in neuronal apoptosis induced by trophic withdrawal. J. Neurosci. **20:** 2567–2574

41 Gleichmann M., Weller M. and Schulz J. B. (2000) Insulin-like growth factor-1-mediated protection from neuronal apoptosis is linked to phosphorylation of the pro-apoptotic protein BAD but not to inhibition of cytochrome c translocation in rat cerebellar neurons. Neurosci. Lett. **282:** 69–72
42 Cheng E. H, Wei M. C., Weiler S., Flavell R. A., Mak T. W., Lindsten T. et al. (2001) BCL-2, BCL-X(L) sequester BH3 domain-only molecules preventing BAX- and BAK-mediated mitochondrial apoptosis. Mol. Cell. **8:** 705–711
43 Condorelli F., Salomoni P., Cotteret S., Cesi V., Srinivasula S. M., Alnemri E. S. et al. (2001) Caspase cleavage enhances the apoptosis-inducing effects of BAD. Mol. Cell. Biol. **21:** 3025–3036
44 Jurgensmeier J. M., Xie Z., Deveraux Q., Ellerby L., Bredesen D. and Reed J. C. (1998) Bax directly induces release of cytochrome c from isolated mitochondria. Proc. Natl. Acad. Sci. USA **95:** 4997–5002
45. Pastorino J. G., Chen S. T., Tafani M., Snyder J. W. and Farber J. L. (1998) The overexpression of Bax produces cell death upon induction of the mitochondrial permeability transition. J. Biol. Chem. **273:** 7770–7775
46 Wands J. R., Mohr L., Banerjee K., Ganju N., Tanaka S. and Monte S. M. de la (in press) Ethanol and IRS-1 protein in the liver and brain. In: Proceedings on Signal Transduction and Alcohol, Lund, Sweeden
47 Urso T., Gavaler J. S. and Van T. D. (1981) Blood ethanol levels in sober alcohol users seen in an emergency room. Life Sci **28:** 1053–1056
48 Nikolic M., Dudek H., Kwon Y. T., Ramos Y. F. and Tsai L. H. (1996) The cdk5/p35 kinase is essential for neurite outgrowth during neuronal differentiation. Genes Dev. **10:** 816–825
49 Monte S. M. de la, Neely T. R., Cannon J. and Wands J. R. (2000) Oxidative stress and hypoxia-like injury cause Alzheimer-type molecular abnormalities in CNS neurons. Cell. Mol. Life Sci. **57:** 1–13
50 Monte S. M. de la, Ganju N., Feroz N., Luong T., Banerjee K., Cannon J. et al. (2000) Oxygen free radical injury is sufficient to cause some Alzheimer-type molecular abnormalities in human CNS neuronal cells. J. Alzheimer Dis. **2:** 1–21
51 Hansen M. B, Nielsen S. E. and Berg K. (1989) Re-examination and further development of a precise and rapid dye method for measuring cell growth/cell kill. J. Immunol. Methods **119:** 203–210
52 Monte S. M. de la, Ganju N. and Wands J. R. (1999) Microtiter immunocytochemical ELISA assay: a novel and highly sensitive method of quantifying immunoreactivity. Biotechniques **26:** 1073–1076
53 Ausubel F. M, Brent R., Kingston R. E., Moore D. D., Seidman J. G., Smith J. A. et al. (2000) Current Protocols in Molecular Biology, Wiley, New York
54 Monte S. M. de la, Ganju N., Tanaka S., Banerjee K., Karl P. J., Brown N. V. et al. (1999) Differential effects of ethanol on insulin-signaling through the insulin receptor substrate-1. Alcohol Clin. Exp. Res. **23:** 770–777
55 Jedrzejewska A. and Wierzba-Bobrowicz T. (1990) Ultrastructure of ventral hippocampus of rat with chronic ethanol intoxication. Zentralbl. Allg. Pathol. **136:** 359–366
56 Tavares M. A. and Paula-Barbosa M. M. (1983) Mitochondrial changes in rat Purkinje cells after prolonged alcohol consumption: a morphologic assessment. J. Submicrosc. Cytol. **15:** 713–720
57 Alexander B. M., Dugast I., Ercolani L., Kong X. F., Giere L. and Nasrin N. (1992) Multiple insulin-responsive elements regulate transcription of the GAPDH gene. Adv. Enzyme Regul. **32:** 149–159
58 Monte S. M. de la, Sohn Y. K., Ganju N. and Wands J. R. (1998) P53- and CD95-associated apoptosis in neurodegenerative diseases. Lab Invest **78:** 401–411
59 Xiang H. (1998) Bax involvement in p53-mediated neuronal cell death. J. Neurosci. 18: 1363–1373
60 Ueno H., Honda H., Nakamoto T., Yamagata T., Sasaki K., Miyagawa K. et al. (1997) The phosphatidylinositol 3′ kinase pathway is required for the survival signal of leukocyte tyrosine kinase. Oncogene **14:** 3067–3072
61 Manchem V. P., Goldfine I. D., Kohanski R. A., Cristobal C. P., Lum R. T., Schow S. R. et al. (2001) A novel small molecule that directly sensitizes the insulin receptor in vitro and in vivo. Diabetes 50: 824–830
62 Yokoyama I., Yonekura K., Moritan T., Tateno M., Momose T., Ohtomo K. et al. (2001) Troglitazone improves whole-body insulin resistance and skeletal muscle glucose use in type II diabetic patients. J. Nucl. Med. 42: 1005–1010